Toward Single-Cell Analysis by Plume Collimation in Laser Ablation Electrospray Ionization Mass Spectrometry

ARTICLE *in* ANALYTICAL CHEMISTRY · FEBRUARY 2013

Impact Factor: 5.64 · DOI: 10.1021/ac303347n · Source: PubMed

2 AUTHORS:

Jessica A Stolee
George Washington University
10 PUBLICATIONS **133** CITATIONS

SEE PROFILE

Akos Vertes
George Washington University
194 PUBLICATIONS **4,634** CITATIONS

SEE PROFILE

analytical chemistry

Article

pubs.acs.org/ac

Toward Single-Cell Analysis by Plume Collimation in Laser Ablation Electrospray Ionization Mass Spectrometry

Jessica A. Stolee and Akos Vertes*

Department of Chemistry, W. M. Keck Institute for Proteomics Technology and Applications, The George Washington University, Washington, District of Columbia 20052, United States

Supporting Information

ABSTRACT: Ambient ionization methods for mass spectrometry have enabled the in situ and in vivo analysis of biological tissues and cells. When an etched optical fiber is used to deliver laser energy to a sample in laser ablation electrospray ionization (LAESI) mass spectrometry, the analysis of large single cells becomes possible. However, because in this arrangement the ablation plume expands in three dimensions, only a small portion of it is ionized by the electrospray. Here we show that sample ablation within a capillary helps to confine the radial expansion of the plume. Plume collimation, due to the altered expansion dynamics, leads to greater interaction with the electrospray plume resulting in increased ionization efficiency, reduced limit of detection (by a factor of ~13, reaching 600 amol for verapamil), and extended dynamic range (6 orders of magnitude) compared to conventional LAESI. This enhanced sensitivity enables the analysis of a range of metabolites from small cell populations and single cells in the ambient environment. This technique has the potential to be integrated with flow cytometry for high-throughput metabolite analysis of sorted cells.

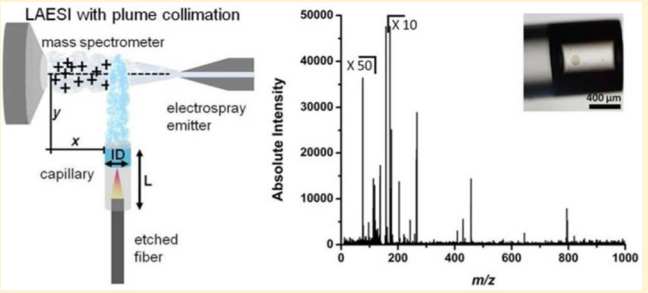

The analysis of metabolite distributions in biological systems can give insight into the physiological and disease states of an organism and is critical to understanding its response to environmental stimuli and drugs. However, the detection of the over ~2700 currently known metabolites present in the human metabolome at widely varying concentrations requires the use of a high-throughput technique that can analyze physically and chemically diverse small molecules.[1] Due to the selectivity and quantitative capabilities of mass spectrometry, it has become an indispensable tool in the emerging field of metabolomics.[2,3]

Compositional heterogeneity within cell populations can be used to characterize different phenotypes on fewer and fewer cells, ultimately at the single-cell level.[4] New cell isolation methods, such as laser capture microdissection, are being developed to extract cells prior to chemical analysis by mass spectrometry.[5] Mass spectrometric techniques for single-cell analysis include matrix-assisted laser desorption ionization, secondary ion mass spectrometry that has been used to image the subcellular distributions of lipids, and capillary electrophoresis coupled with electrospray ionization (ESI) that has enabled the analysis of metabolites from single neurons.[6−8] While these methods facilitate the use of mass spectrometry for single-cell analysis, they require elaborate sample preparation and cannot follow the dynamic processes involved in cellular metabolism. Thus, techniques with in situ capabilities, high sensitivity, and a wide range of quantitation are becoming increasingly important.

To obtain an accurate snapshot of the metabolite profiles in a sample, extensive efforts are being devoted to developing ionization techniques for the rapid analysis of biological specimens in their native environment.[9] Since the introduction of desorption electrospray ionization (DESI)[10] in 2004, numerous ambient ion sources have emerged ranging from those based on spray extraction, e.g., DESI, to plasma sampling and ionization, e.g., direct analysis in real time (DART),[11] to laser based techniques, e.g., laser ablation electrospray ionization (LAESI),[12] among a host of others.[13]

Some ambient methods, e.g., LAESI, currently show promise for in situ single-cell analysis. Optical fibers provide a convenient and robust method for microsampling by laser pulses. When an etched optical fiber was used to deliver laser energy to a sample in LAESI, the analysis of large single cells with an average volume of ~1 nL became possible.[14] This technique provided information on coexisting cell phenotypes and their metabolic differences in heterogeneous populations.[15,16] However, due to their minute sample volumes (as low as a few femtoliters) and the limited number of some molecules, the analysis of smaller cells becomes more challenging.

LAESI utilizes 2.94 μm wavelength laser radiation that is strongly absorbed by the native water content present in

Received: November 19, 2012
Accepted: February 28, 2013
Published: February 28, 2013

biological samples. Rapid energy deposition by a pulsed laser in the ambient environment initiates surface evaporation, shock-wave emission, and, at elevated fluences, phase explosion.[17,18] These processes result in a radially expanding plume of vapor and fine droplets originating from the sample that is ionized by an electrospray plume of highly charged droplets. Because the ablation plume expands in three dimensions, only a small portion of it is ionized by the electrospray plume, resulting in low ionization efficiencies.

Here we present sample ablation experiments performed in a capillary to minimize the radial expansion of the ablation plume. We demonstrate that by altering the ablation plume dynamics we are able to achieve higher ion yields and increased sensitivity, probably due to an improved overlap with the electrospray plume. Plume collimation in LAESI enables the detection of metabolites from small populations of human and animal cells including single cells from the latter. We use a diverse group of cells to demonstrate the feasibility of this method, including β-cells derived from the rat pancreas that are responsible for insulin secretion and are important in diabetes, epithelial cells from the buccal mucosa of a human, megakaryoblast cells derived from the human bone marrow, and individual sea urchin eggs. Biologically relevant metabolites are detected from these diverse set of cells.

MATERIALS AND METHODS

Plume Collimation in Laser Ablation Electrospray Ionization. Mass spectrometry experiments were conducted in positive ion mode with orthogonal acceleration time-of-flight mass spectrometers. Small cell populations were studied on a Q-TOF Premier instrument, whereas the single-cell experiments were conducted on a Synapt G2-S system (Waters CO., Milford, MA). Both of them were equipped with a home-built electrospray system described elsewhere.[12] Briefly, a syringe pump (Physio 22 or 11 Plus, Harvard Apparatus, Holliston, MA) was operated to supply 50% methanol solution with 0.1% acetic acid (v/v) to a tapered tip emitter at a rate of 300 nL/min. To make direct comparisons with conventional LAESI, we did not vary the spray conditions. A power supply (PS350, Stanford Research System, Inc., Sunnyvale, CA) was used to apply high voltage to the emitter to generate the electrospray. The emitter was placed on axis with the mass spectrometer orifice, with its tip located 10 to 12 mm away from it. In conventional LAESI, a plano-convex focusing lens was used to focus laser radiation at 2.94 μm wavelength provided by a Nd:YAG laser driven optical parametric oscillator (Opolette 100, Opotek Inc., Carlsbad, CA).

In the plume collimation experiments, laser radiation was delivered through a germanium oxide (GeO_2) optical fiber (450 μm core diameter, HP Fiber, Infrared Fiber Systems, Inc., Silver Spring, MD) with a tip etched in a 2% nitric acid solution as described earlier.[14] Optical fibers with a 200 μm core diameter were also tested. Borosilicate and quartz capillaries with inner diameters, ID, ranging from 0.6 to 1 mm (Sutter Instrument, Novato, CA), were cleaved to lengths, L, ranging from 2 to 6 mm with a sapphire scribe and used to hold the liquid sample. The capillary was held in place with a fiber clamp (HFF001, Thorlabs, Newton, NJ) and its position was adjusted by a three-axis translation stage. Ablation was performed by inserting the optical fiber tip into the liquid sample that is held inside the capillary, as shown in Figure 1a. The fiber was held by a fiber chuck and positioned with a five-axis translator (BFT-5, Siskiyou Corporation, Grants Pass, OR). Similar to conventional LAESI, the ablation products were ionized by an electrospray.

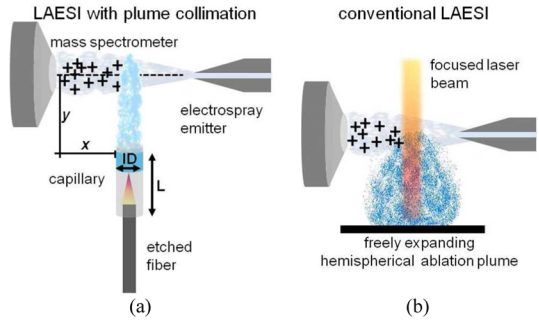

Figure 1. (a) Schematic top view of LAESI with plume collimation. An etched optical fiber is inserted into a glass capillary of inner diameter, ID, and length, L, that contains the sample. Upon ablation in the capillary, a collimated plume emerges (shown in blue) and is ionized by an electrospray. Ablation in the capillary leads to a forward directed plume. (b) Schematic side view of conventional LAESI. The laser beam is focused by a lens onto the sample. Due to the hemispherical expansion of the ablation plume, only a small portion of it is intercepted by the electrospray.

Chemicals. HPLC grade methanol and water were purchased from Alfa Aesar (Ward Hill, MA) and acetic acid was purchased from Fluka (St. Louis, MO). Verapamil, bradykinin, and reserpine were purchased from Sigma Aldrich (St. Louis, MO) and stock solutions were prepared in 50% methanol.

Cell Culturing and Sampling. Epithelial β-cells (RIN5mF) from the rat pancreas were kindly provided by Aleksander Jeremic of the George Washington University and megakaryoblast cells (MEG-01) were purchased from ATCC (CRL-2021, Manassas, VA). Cell lines were maintained in RPMI 1640 medium supplemented with 10% fetal bovine serum and 1% penicillin-streptomycin (ATCC, Manassas, VA) in a 5% humidity controlled incubator at 37 °C. Prior to experiments, β-cells were detached from the culture dish with trypsin-EDTA (Invitrogen, Grand Island, NY) and suspended in medium. To minimize their interference in the mass spectra, the medium was removed, and the β-cells were suspended in a 10× diluted phosphate buffered saline (PBS) solution. Prior to experiments the number of cells in the capillary was determined under a microscope. Human buccal mucosa epithelial cells were collected from a healthy subject. For the experiments with the megakaryoblast cells, the medium was removed and the cells were suspended in 10× diluted PBS solution.

Single-Cell Experiments. Unfertilized sea urchin eggs (*Lytechinus pictus*) kept frozen at −80 °C in artificial seawater were revived and diluted in HPLC water. The sea urchin eggs did not visibly lyse. Single sea urchin eggs were extracted from the solution by using a manually pulled glass capillary with an inner diameter of ∼90 μm that was held and controlled by a microdissection system (TransferMan NK2 and CellTram Air, Eppendorf, Hauppauge, NY). The selected cell was deposited into a 0.5-μL droplet of HPLC water and the droplet containing the cell was subsequently pipetted into a capillary for the plume collimation LAESI experiments.

RESULTS AND DISCUSSION

Plume Collimation: Controlling Factors. In the plume collimation experiments the capillary length and diameter, the position of the capillary relative to the electrospray and mass

dx.doi.org/10.1021/ac303347n | Anal. Chem. 2013, 85, 3592−3598

spectrometer orifice, and the fiber parameters were systematically varied to obtain optimal ion yields. With use of verapamil and bradykinin solution samples, it was found that the capillary length, which ranged from 2 to 8 mm, and the inner diameter, which ranged from 0.6 to 1 mm, had minimal impact on the ion intensities. As the inner diameter of the capillary was reduced to 500 μm, i.e., it approached the 450 μm outer diameter of the optical fiber, the ion signal increased (see Figure S2 in the Supporting Information). It was, however, difficult to insert the fiber into the capillary without breaking it. Therefore, it was easiest to work with capillaries having inner diameters of 750 μm or larger. The fiber tip was inserted approximately 200 μm into the sample solution prior to the onset of ablation.

The schematics in Figure 1 illustrate the major differences between the plume collimation and conventional LAESI experiments. Collimation within the capillary results in a quasi-one-dimensional plume expansion (see Figure 1a), whereas conventional LAESI (depicted in Figure 1b) yields a freely expanding hemispherical ablation plume. Because of the limited volume of the collimated plume, the position of the capillary relative to the electrospray had a strong effect on the signal intensity. The capillary and the electrospray emitter were kept in the same plane by maintaining their elevation equal in the z direction and the intercept of their axes located approximately 4−5 mm from the mass spectrometer orifice (see x in Figure 1a). The end of the capillary was approximately 10 mm away from the intercept (see y in Figure 1a). This position provided the highest verapamil signal intensities probably due to the maximum overlap between the two plumes. Moving away from the optimized geometry, the signal intensities decreased by up to 2 orders of magnitude or became undetectable.

In the plume collimation experiments, an etched optical fiber tip is used to deliver the laser energy into the sample. We also explored how the sharpness of the fiber tip affected the ablation in the capillary. It was found that a flat, cleaved fiber end did not deliver sufficient energy for the ablation of the sample. Sharp fibers, with approximately 20 μm tip diameters, provided the best energy coupling for ablation.

Analytical Figures of Merit for Plume Collimation versus Conventional LAESI. To discover the effects of plume collimation on the figures of merit, we compared the measured ion intensities with that of conventional LAESI for a range of analyte concentrations. Solutions of verapamil were prepared in 50% methanol with 0.1% acetic acid from a stock solution of 1.2 mM. A droplet of ~0.5 μL was deposited inside a capillary with an inner diameter of 750 μm. An optical fiber with a tip diameter of ~20 μm was used to deliver laser pulses with 20 Hz repetition rate to the sample until the entire sample was ablated. The mass of the capillary was measured with a semimicrobalance (MS105DU, Mettler Toledo, Columbus, OH) before and after experiments to account for any sample residue remaining in the capillary. A new capillary was used for every solution, and each measurement was repeated three times. Mass spectra obtained during the ablation were averaged and the intensity of the molecular ion was recorded.

The mass spectra in the plume collimation experiments were very similar to the conventional LAESI-MS results (see Figure S3 in the Supporting Information). As shown in Figure 2, the limit of detection for verapamil using LAESI with plume collimation was at 1.2×10^{-9} M concentration, which corresponds to 600 attomoles of analyte. The inset in Figure 2 shows that at the limit of detection, the signal-to-noise ratio is

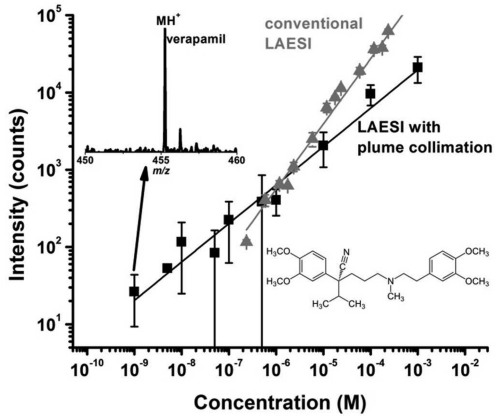

Figure 2. Verapamil ion intensities as a function of solution concentration measured by LAESI with plume collimation (in black) and conventional LAESI (in gray; from ref 12). Plume collimation enables the detection of verapamil with a dynamic range of 6 orders of magnitude versus 4 decades for conventional LAESI. As shown in the inset, at the limit of detection the molecular ion of verapamil exhibits a signal-to-noise ratio greater than 3.

greater than 3. By using linear regression, a correlation coefficient of 0.986 was obtained. This limit of detection is 13 times lower than the value found for conventional LAESI that exhibits a limit of detection of 8 fmol measured at 2.4×10^{-7} M concentration. Furthermore, LAESI with plume collimation exhibits a dynamic range extended to 6 orders of magnitude versus the 4 decades found for conventional LAESI. Similar results were found for reserpine (see Figure S1 in the Supporting Information) and bradykinin. For these two compounds, the lowest detected concentration was 1.0×10^{-8} M, significantly below the 7.5×10^{-7} M value found for reserpine with conventional LAESI.[12]

These greatly improved figures of merit are, in part, attributed to delivering more of the ablated sample into the electrospray plume for enhanced ion production. Similar results were obtained with other analytes, such as reserpine and bradykinin. To test the utility of the improved sensitivity, cell populations of diminishing size were analyzed.

Analysis of Mammalian Cells. In situ mass spectrometric analysis of mammalian cells was performed by using LAESI with plume collimation. Microscope observations at various stages of handling, including inside the capillary, indicated that the cells remained intact until the ablation. The culture medium was separately analyzed and the corresponding signal was subtracted as background from the cell sample spectra. Apart from the obvious advantage of better sensitivity, using a capillary to hold the sample has a few additional benefits. The presence of water is a prerequisite for sample ablation in LAESI. Since in these experiments the cells are suspended in a droplet and held in a capillary, the evaporation rate is significantly decreased compared to conventional LAESI. This allows for the analysis of smaller sample volumes resulting in reduced dilution of the cell contents by the suspending medium. Furthermore, because of the improved sensitivity, a cell suspension, rather than a cell pellet, can be used for analysis.

Potential metabolites from mammalian cells were identified by using the accurate mass of the monoisotopic peak, isotope distributions, and literature searches.

Rat insulinoma β-cells (RIN5mF) with an average cell diameter of 10 μm, corresponding to a single-cell volume of

dx.doi.org/10.1021/ac303347n | Anal. Chem. 2013, 85, 3592−3598

~500 fL/cell, were analyzed with LAESI mass spectrometry utilizing plume collimation. Figure 3a shows a spectrum

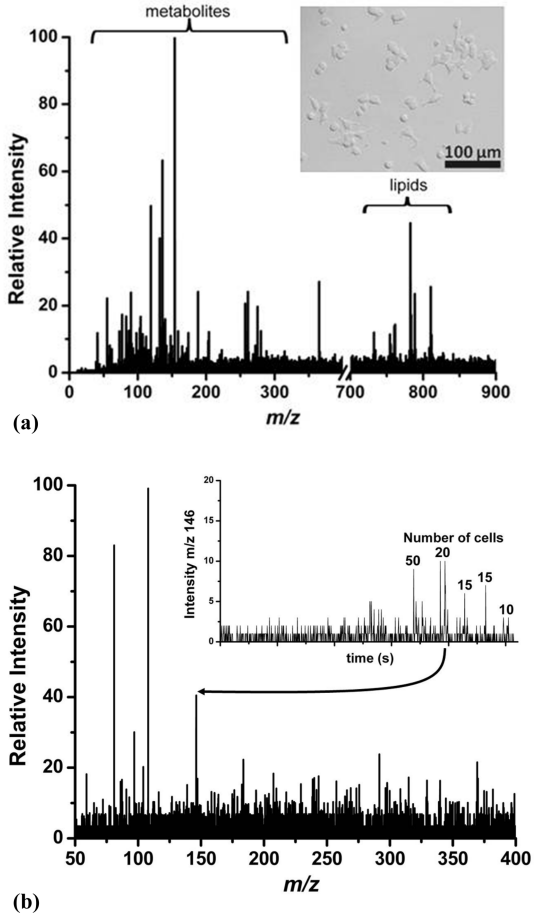

Figure 3. (a) A representative mass spectrum obtained from <100 epithelial β-cells from rat insulinoma by LAESI with plume collimation. The spectrum exhibits a large number and variety of peaks. Tentative identification of metabolites and lipids is given in Table S1 of the Supporting Information. Many of these peaks were also detected in larger cell populations. Microscope image in the inset shows β-cells which are ~10 μm in diameter. (b) A mass spectrum from <20 megakaryoblast cells. The inset shows the selected ion chromatogram of the spermidine ion at m/z 146.15 detected in samples containing 50 to 10 cells.

obtained from fewer than 100 β-cells, corresponding to a total cell volume of ~50 pL, suspended in a 0.5 μL droplet of diluted PBS buffer solution. Similar to conventional LAESI, singly charged protonated and potassiated ions were primarily observed. Approximately 35 ions were detected from this sample and more than half of the small molecules have been tentatively assigned to biologically relevant metabolites such as primary amino acids (e.g., alanine at m/z 90.04 and proline at m/z 116.05), nucleobases (e.g., uracil at m/z 135.01 and adenine at m/z 174.02), and phospholipids (e.g., phosphatidylcholine PC(33:2) at m/z 782.53). As expected, a greater number of metabolites were detected with higher signal intensities from more concentrated cell suspensions. Since these cells are adherent, they have an affinity to the inner wall of the capillary and many of them remained there even after ablation. This made the analysis of fewer than 100 cells difficult.

Megakaryoblast cells (MEG-01) that primarily grow in suspension have a lower affinity to the inner wall of the capillary than β-cells. While some of the adherent megakaryoblast cells are large, with diameters up to 50 μm, the average cell diameter of a suspended cell is 18 μm (corresponding to a single-cell volume of ~3 pL/cell). With use of plume collimation in LAESI, signal was obtained from as few as 20 megakaryoblast cells or a total cell volume of ~60 pL (see the spectrum in Figure 3b). In this small cell population, spermidine, at m/z 146.15, was one of the significant peaks. Its selected ion chromatogram is shown in the inset of Figure 3b. It can be observed that as the number of cells is decreased from 50 to 10 the intensity of this ion also decreases. Other peaks that were detected in larger cell populations include spermine (m/z 203.22) and phospholipids (e.g., phosphatidylcholine PC(36:4) at m/z 782.48).

Toward Single-Cell Analysis. Buccal epithelial cells are somewhat larger than typical mammalian cells, with sizes ranging from 30 to 50 μm that, assuming spherical shape, corresponds to volumes of 14 to 65 pL/cell. To produce a sample with a small cell population, a dense cell suspension was diluted in water until the desired concentration was reached. There was no observable cell lysis when the cells were diluted in water. Figure 4a shows the signal obtained from the detection of 6 cheek cells (a total cell volume of 84 to 390 pL) enabled by plume collimation. Many of the detected metabolites have been tentatively assigned to metabolites present in a typical diet or those involved in the gut

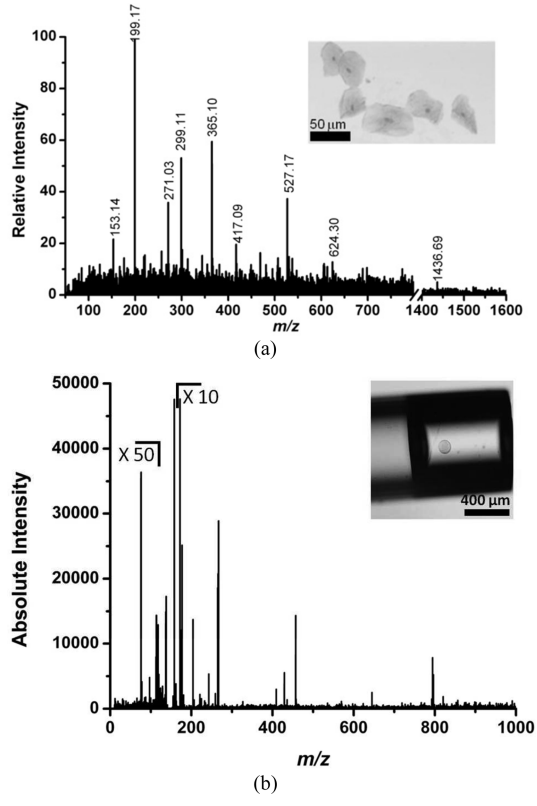

Figure 4. (a) Mass spectrum obtained by LAESI with plume collimation from six cheek cells contained in water. Tentative assignment of 7 significant peaks is given in Table S2 of the Supporting Information. These peaks were also detected in larger cell populations. The inset shows a microscope image of the cheek cells. (b) Mass spectrum of a single sea urchin egg by LAESI with plume collimation. The inset shows the image of a single egg in the capillary before ablation.

dx.doi.org/10.1021/ac303347n | Anal. Chem. 2013, 85, 3592−3598

metabolism. For example, peaks at m/z 219.01, 365.10, and 527.17 have been tentatively assigned to a hexose, a disaccharide, and a trisaccharide, respectively. However, the obtained spectra exhibited day-to-day variations, probably due to differences in diet, thus for this study it is more appropriate to have cells that are cultured in a controlled environment.

Frozen sea urchin eggs, with diameters of 90 to 100 μm or volumes of 400 to 500 pL, were thawed and diluted in HPLC water. Individual sea urchin eggs were selected by using the micromanipulator system and deposited into a capillary for LAESI mass spectrometry with plume collimation. Peaks corresponding to the electrospray background and HPLC water were subtracted from the sea urchin egg spectrum. Numerous ions were detected from a single sea urchin egg (see Figure 4b). Certain regions of the spectrum, i.e., m/z <137 and >160, were enlarged to indicate the number of peaks present. Some of the peaks have been tentatively assigned to metabolites such as glycine (m/z 76.04), trimethylamine dimer (m/z 141.14), and lipids (e.g., doubly charged phosphatidylcholine PC(35:4) or PC(36:3) at m/z 403.76 and doubly charged phosphatidylserine PS(38:7) or PS(37:0) at m/z 422.73) that are known to be abundant in sea urchin eggs.[19] As these cells are much larger in volume than a typical animal cell, for the analysis of the latter further improvements in sensitivity are needed.

Plume Dynamics. During the ablation process in LAESI a plume of particulates, droplets, and vapor is formed. It appears that the angular distribution of the expanding ablation plume has a strong effect on the ion intensity. To understand the mechanistic differences contributing to the increased ionization efficiencies due to plume collimation, we compare the ablation plume dynamics with that of conventional LAESI.

When a nanosecond mid-IR laser pulse of sufficient fluence impinges on an aqueous sample, the nonlinear absorption of the laser radiation by water initiates surface evaporation, shock-wave emission, and the ejection of fine droplets via phase explosion.[20−22] The first stage, i.e., surface evaporation, results in a relatively slow plume expansion.[18,22,23] Material removal due to this process is not very efficient. However, during phase explosion, i.e., when the target is superheated close to its critical temperature, a rapidly expanding plume of vapor, droplets, and particulate matter is ejected. For example, a 70 ns laser pulse with 2.94 μm wavelength and 5.4 J/cm^2 fluence induces phase explosion at ∼120 ns.[18] After ∼1 μs, the phase explosion induced recoil pressure results in an efficient secondary material ejection process.

In conventional LAESI, the ablation plume is free to expand in three dimensions. The interaction of the ablation products with the electrospray plume has been studied by using fast imaging by flash shadowgraphy.[12] Images show a radially expanding ablation plume in which only a small fraction of the droplets are intercepted by the electrospray plume. It has been estimated that droplets with an effective diameter of 5 μm result in the best interaction with the electrospray droplets which range from 5 to 10 μm in LAESI experiments.[24,25] Time-resolved imaging experiments show a dependence of droplet bouncing, coalescence, and separation on the size ratio of the two droplets and the Weber number, a dimensionless quantity dependent on the ratio of kinetic to surface energy.[26]

During confined ablation, such as that in the plume collimation experiments, the radial expansion of the plume is hindered and the plume dynamics is altered. As a consequence, increased pressures and temperatures within the target are reached. The ablation by fiber-transmitted laser pulses in a liquid environment has been a topic of interest due to the implications for medical applications.[27−31] These studies found that the fiber tip generates acoustic radiation that causes significant tensile stress in the water and leads to explosive vaporization, cavitation, and bubble formation.[28,29] The collapse of the generated bubbles can result in the ejection of a high-speed liquid jet, and the disruption of tissue in front of the tip.[30,32,33]

To explore the sample ejection in the plume collimation experiments, images were captured at 5 frames/s during the ablation of water in a 750 μm inner diameter capillary by mid-IR laser pulses with 20 Hz repetition rate delivered by an etched optical fiber (see Figure 5). The captured images reveal

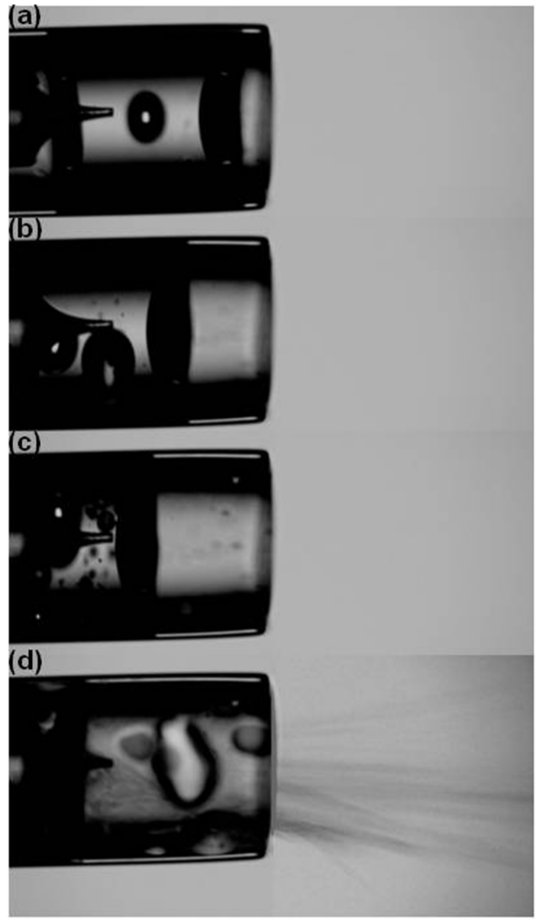

Figure 5. Images show the mid-IR laser ablation of water in a capillary with an inner diameter of 750 μm by an etched optical fiber. Panels a−d show sequential images of bubble formation, collapse, and the ejection of liquid from the capillary.

bubble formation and collapse followed by the ejection of liquid jets and droplets. Figure 5a shows the formation of a bubble in the droplet of water after the laser is turned on. In Figure 5b, another bubble is visible and the initial bubble is starting to collapse. Figure 5c indicates that one of the large bubbles has collapsed and smaller bubbles have formed. This is followed by the ejection of liquid jets, as shown in Figure 5d. In the right half of the image the contrast is increased so that the ejection of the liquid jets can be visualized. At other times during the ablation small droplets are expelled from the capillary (not shown). Side jets were also occasionally observed. Due to the

dx.doi.org/10.1021/ac303347n | Anal. Chem. 2013, 85, 3592−3598

low resolution and long exposure time of these images, it is difficult to discern the diameter of the ejected droplets, but they are measured to be less than 10 μm. It is also important to note that only the largest droplets were captured in these images and it is assumed that much smaller droplets are also being ejected. These large observable droplets are comparable in size to the 5 to 10 μm electrospray droplets, promoting efficient droplet coalescence.

CONCLUSIONS

Conventional LAESI had been successfully used to analyze large populations of mammalian cells and individual plant cells with volumes greater than 1 nL. However, because the ablation plume is free to expand in all three dimensions, conventional LAESI is characterized by significant sample losses and low ionization efficiencies. Here we showed that by performing confined ablation within a capillary, we could achieve higher sensitivity for LAESI ionization. This resulted in lower limits of detection.

The applicability of this technique for the in situ analysis of small cell populations was demonstrated for a diverse group of cell types. In typical ambient ionization mass spectrometry experiments a large cell population ($\sim 10^6$ cells) or a large cell volume (on the nanoliter scale) is required to obtain strong signal. In these experiments, we demonstrated the analysis of small cell populations, corresponding to ~50 pL of cells, and a large single cell by plume collimation in LAESI.

The improved analytical figures of merit are attributed to a better overlap between the collimated ablation plume and the electrospray. In confined liquid ablation, bubble formation and collapse leads to the ejection of sample related droplets and liquid jets. Future experiments with high-speed photography can shed light on the ablation mechanism in plume collimation and can also give insight into the interaction between the ablation plume and the electrospray. The laser energy deposited through the fiber may also have an effect on the produced droplet size, which in turn will impact the percentage of droplets that coalesce with the electrospray plume. Imaging experiments can be used to optimize the interaction between the two plumes for even higher ionization efficiency.

To produce a more confined plume, the capillary and fiber dimensions can be reduced. This will also enable the analysis of reduced sample volumes. A problem related to using a capillary to hold the sample is the adhesion of the sample to the inner wall. This problem is further exaggerated if smaller sample volumes are used, where even minimal sample losses are significant. Capillaries with different surface properties or derivatized capillaries can be used to decrease the interaction with the sample and ensure that all or most of the material is ablated from the capillary.

Our experiments show that higher ionization efficiencies are necessary to move toward the routine mass spectrometric analysis of single mammalian cells in the ambient environment. Plume collimation in LAESI shows promise in advancing this field. Although the confined ablation geometry requires suspended cell samples and precludes tissue imaging applications, it opens up new possibilities in rapid cell analysis. With further optimization, plume collimation in LAESI has the potential to be coupled with flow cytometry for high-throughput single-cell analysis.

ASSOCIATED CONTENT

Supporting Information

Additional information as noted in the text. This material is available free of charge via the Internet at http://pubs.acs.org.

AUTHOR INFORMATION

Corresponding Author

*E-mail: vertes@gwu.edu. Phone: +1 (202) 994-2717. Fax: +1 (202) 994-5873.

Notes

The authors declare no competing financial interest.

ACKNOWLEDGMENTS

The authors acknowledge financial support from the U.S. National Science Foundation under Grant No. CHE-1152302, the George Washington University Selective Excellence Fund, and the Achievement Rewards for College Scholarships. We thank Infrared Fiber Systems, Inc. (Silver Spring, MD) for providing us with the GeO_2 fibers used in this study.

REFERENCES

(1) Duarte, N. C.; Becker, S. A.; Jamshidi, N.; Thiele, I.; Mo, M. L.; Vo, T. D.; Srivas, R.; Palsson, B. O. *Proc. Natl. Acad. Sci. U.S.A.* **2007**, *104*, 1777−1782.
(2) Dettmer, K.; Aronov, P. A.; Hammock, B. D. *Mass Spectrom. Rev.* **2007**, *26*, 51−78.
(3) Bedair, M.; Sumner, L. W. *TrAc, Trends Anal. Chem.* **2008**, *27*, 238−250.
(4) Amantonico, A.; Urban, P. L.; Zenobi, R. *Anal. Bioanal. Chem.* **2010**, *398*, 2493−2504.
(5) Xu, B. G. J.; Caprioli, R. M. *J. Am. Soc. Mass. Spectrom.* **2002**, *13*, 1292−1297.
(6) Ostrowski, S. G.; Van Bell, C. T.; Winograd, N.; Ewing, A. G. *Science* **2004**, *305*, 71−73.
(7) Amantonico, A.; Oh, J. Y.; Sobek, J.; Heinemann, M.; Zenobi, R. *Angew. Chem., Int. Ed.* **2008**, *47*, 5382−5385.
(8) Nemes, P.; Knolhoff, A. M.; Rubakhin, S. S.; Sweedler, J. V. *Anal. Chem.* **2011**, *83*, 6810−6817.
(9) Nemes, P.; Vertes, A. *TrAc, Trends Anal. Chem.* **2012**, *34*, 22−34.
(10) Takats, Z.; Wiseman, J. M.; Gologan, B.; Cooks, R. G. *Science* **2004**, *306*, 471−473.
(11) Cody, R. B.; Laramee, J. A.; Durst, H. D. *Anal. Chem.* **2005**, *77*, 2297−2302.
(12) Nemes, P.; Vertes, A. *Anal. Chem.* **2007**, *79*, 8098−8106.
(13) Harris, G. A.; Galhena, A. S.; Fernandez, F. M. *Anal. Chem.* **2011**, *83*, 4508−4538.
(14) Shrestha, B.; Vertes, A. *Anal. Chem.* **2009**, *81*, 8265−8271.
(15) Shrestha, B.; Nemes, P.; Vertes, A. *Appl. Phys. A: Mater. Sci. Process.* **2010**, *101*, 121−126.
(16) Shrestha, B.; Patt, J. M.; Vertes, A. *Anal. Chem.* **2011**, *83*, 2947−2955.
(17) Vogel, A.; Venugopalan, V. *Chem. Rev.* **2003**, *103*, 577−644.
(18) Chen, Z. Y.; Vertes, A. *Phys. Rev. E: Stat., Nonlinear, Soft Matter Phys.* **2008**, 77.
(19) Kubo, H.; Irie, A.; Inagaki, F.; Hoshi, M. *J. Biochem.* **1990**, *108*, 185−192.
(20) Kelly, R.; Miotello, A. *Phys. Rev. E: Stat. Phys., Plasmas, Fluids, Relat. Interdiscip. Top.* **1999**, *60*, 2616−2625.
(21) Shori, R. K.; Walston, A. A.; Stafsudd, O. M.; Fried, D.; Walsh, J. T. *IEEE J. Sel. Top. Quantum Electron.* **2001**, *7*, 959−970.
(22) Apitz, I.; Vogel, A. *Appl. Phys. A: Mater. Sci. Process.* **2005**, *81*, 329−338.
(23) Chen, Z. Y.; Bogaerts, A.; Vertes, A. *Appl. Phys. Lett.* **2006**, *89*, 041503.
(24) Nemes, P.; Marginean, I.; Vertes, A. *Anal. Chem.* **2007**, *79*, 3105−3116.

(25) Nemes, P.; Huang, H. H.; Vertes, A. *Phys. Chem. Chem. Phys.* **2012**, *14*, 2501−2507.
(26) Tang, C.; Zhang, P.; Law, C. K. *Phys. Fluids* **2012**, *24*, 022101.
(27) Ith, M.; Pratisto, H.; Altermatt, H. J.; Frenz, M.; Weber, H. P. *Appl. Phys. B: Lasers Opt.* **1994**, *59*, 621−629.
(28) Frenz, M.; Paltauf, G.; SchmidtKloiber, H. *Phys. Rev. Lett.* **1996**, *76*, 3546−3549.
(29) Paltauf, G.; Schmidt-Kloiber, H.; Frenz, M. *J. Acoust. Soc. Am.* **1998**, *104*, 890−897.
(30) Brujan, E. A.; Nahen, K.; Schmidt, P.; Vogel, A. *J. Fluid Mech.* **2001**, *433*, 251−281.
(31) Paltauf, G.; Dyer, P. E. *Chem. Rev.* **2003**, *103*, 487−518.
(32) Brujan, E. A.; Nahen, K.; Schmidt, P.; Vogel, A. *J. Fluid Mech.* **2001**, *433*, 283−314.
(33) Palanker, D.; Vankov, A.; Miller, J.; Friedman, M.; Strauss, M. *J. Appl. Phys.* **2003**, *94*, 2654−2661.

Supporting Information for

Toward Single Cell Analysis by Plume Collimation in Laser Ablation Electrospray Ionization Mass Spectrometry

*Jessica A. Stolee and Akos Vertes**

Department of Chemistry, W. M. Keck Institute for Proteomics Technology and Applications,

The George Washington University, Washington, District of Columbia 20052

* To whom correspondence should be addressed. E-mail: vertes@gwu.edu. Phone: +1 (202) 994-2717. Fax: +1 (202) 994-5873.

Figure S1. Reserpine ion intensities as a function of solution concentration measured by LAESI with plume collimation (in black) and conventional LAESI (in gray; from Ref. [1]). Extended dynamic range and lower limit of detection is observed with plume collimation. The inset shows the reserpine signal at the limit of detection.

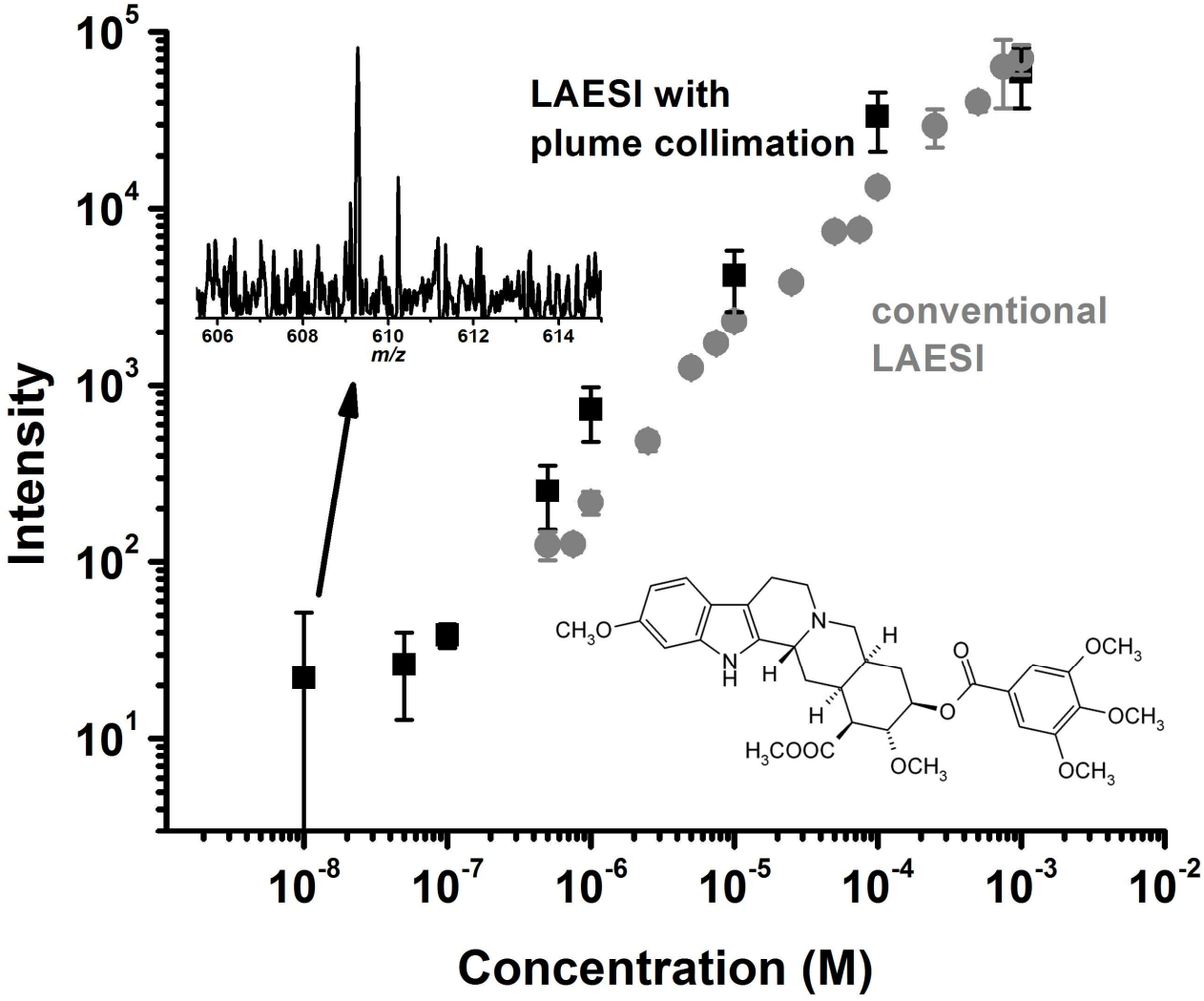

Figure S2. Bradykinin molecular ion signal intensity as a function of the capillary inner diameter in LAESI-MS experiments with plume collimation. Borosilicate and quartz capillaries produced similar results. In the 0.6 to 0.9 mm range there was no significant diameter dependence. As the inner diameter of the capillary was reduced to 0.50 mm, i.e., it approached the 0.45 mm outer diameter of the optical fiber, the ion signal increased. It was, however, difficult to insert the fiber into the capillary without breaking it.

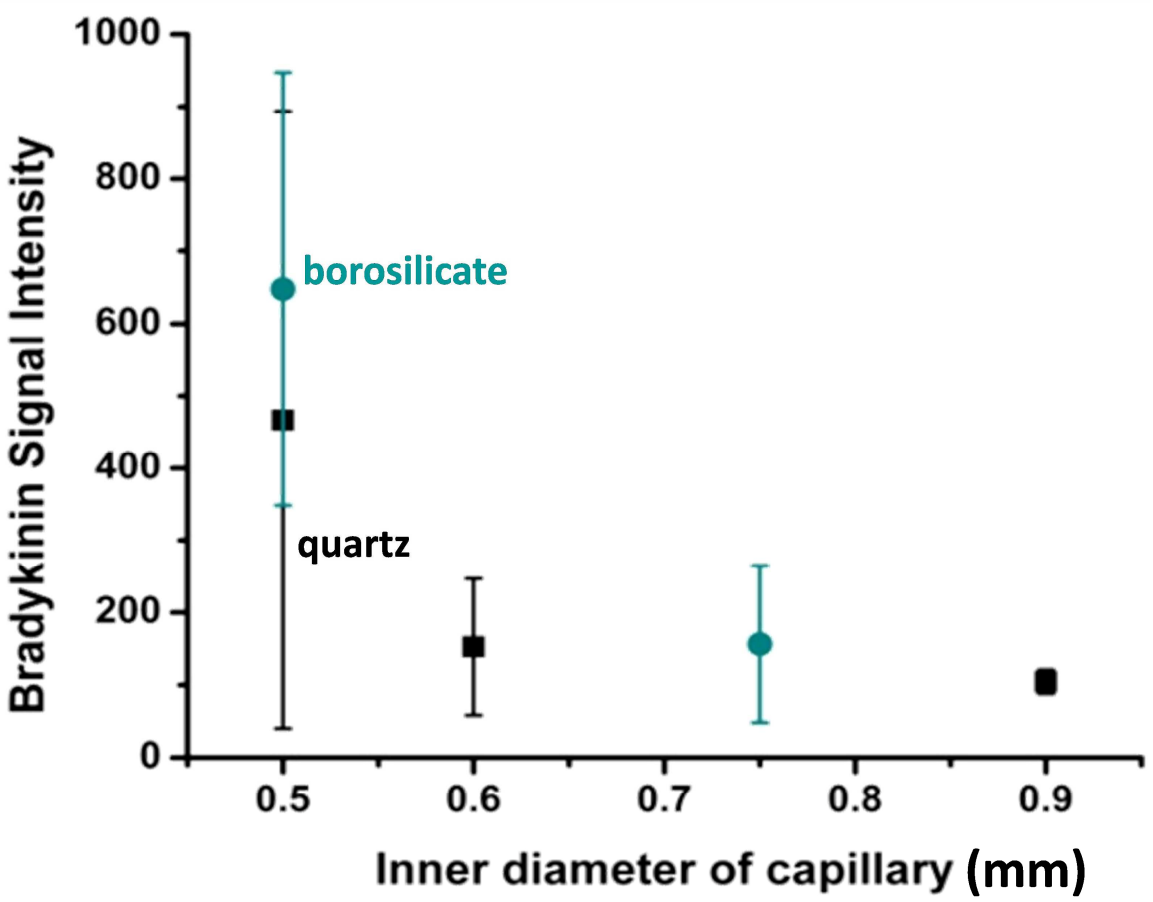

Figure S3. Verapamil mass spectra at two different concentrations, (a) 10^{-5} M and (b) 10^{-7} M, acquired using LAESI with plume collimation. No fragmentation of the verapamil or spectral congestion in the low mass region is observed. The minor peaks in the 10^{-7} M spectrum are related to imperfect background subtraction.

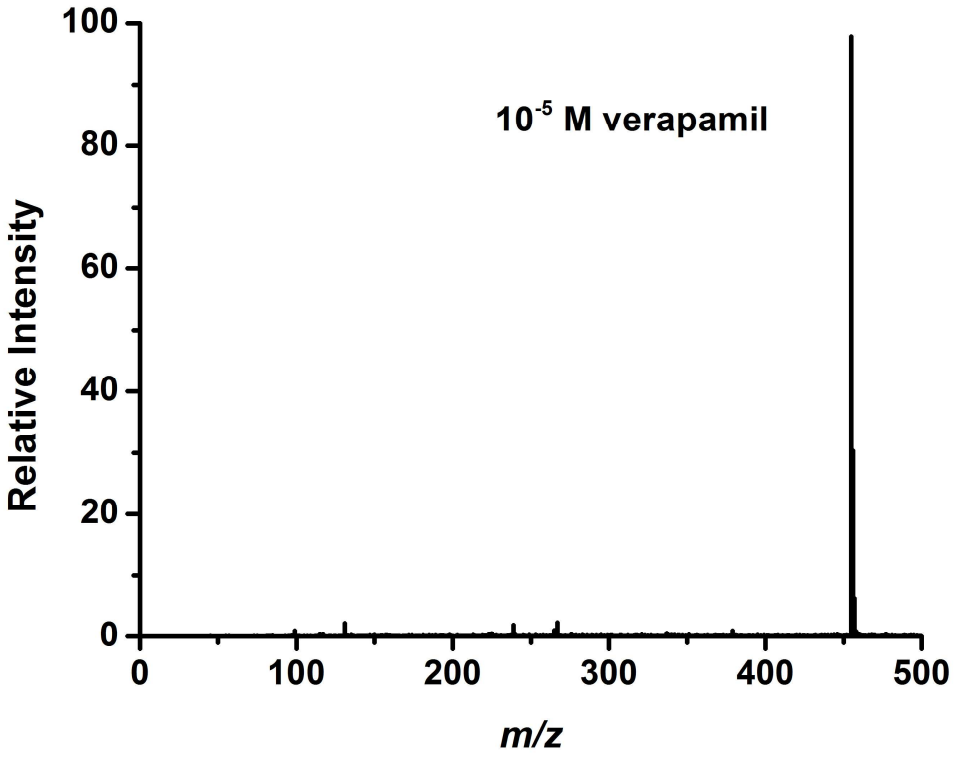

(a)

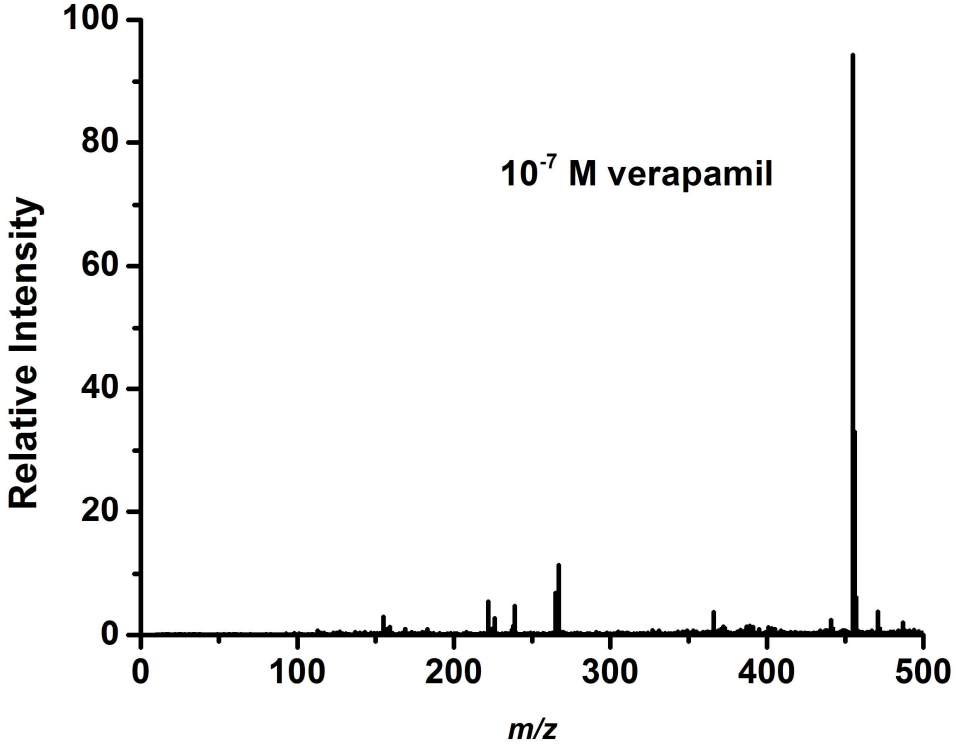

(b)

Table S1. Tentative identification of metabolites and lipids in epithelial β-cells from rat insulinoma based on 26 peaks in LAESI-MS spectra (see Figure 3a) acquired in plume collimation experiments.

Metabolites and Lipids	**Formula**	**Ion**	$m/z_{meas.}$	$m/z_{calc.}$	**Δm (mDa)**
alanine	$C_3H_7NO_2$	$[M+H]^+$	90.0397	90.0550	-15.3
guanidine	CH_5N_3	$[M+K]^+$	98.0127	98.0115	1.2
methylguanidine / alanine	$C_2H_7N_3$	$[M+K]^+$	112.0225	112.0272	-4.7
	$C_3H_7NO_2$	$[M+Na]^+$		112.0369	-14.4
proline	$C_5H_9NO_2$	$[M+H]^+$	116.0467	116.0706	-23.9
succinic acid	C_4H6O_4	$[M+H]^+$	119.0440	119.0339	10.1
propionylglycine / hydroxyproline / creatine	$C_5H_9NO_3$	$[M+H]^+$	132.0745	132.0655	-9.0
	$C_4H_9N_3O_2$	$[M+H]^+$		132.0768	2.3
uracil	$C_4H_4N_2O_2$	$[M+Na]^+$	135.0103	135.0165	6.2
creatinine / cysteine	$C_4H_7N_3O$	$[M+Na]^+$	136.0467	136.0481	1.4
	$C_4H_9NO_2S$	$[M+H]^+$		136.0427	-4.0
spermidine	$C_7H_{19}N_3$	$[M+H]^+$	146.1660	146.1652	-0.8
methionine	$C_5H_{11}NO_2S$	$[M+H]^+$	150.0414	150.0583	16.9
creatine	$C_4H_9N3O_2$	$[M+Na]^+$	154.0685	154.0587	-9.8
hypoxanthine	$C_5H_4N_4O$	$[M+Na]^+$	159.0206	159.0277	7.1
cysteic acid / amino-phosphonopropionic acid / creatine / propionylglycine	$C_3H_7NO_5S$	$[M+H]^+$	170.0211	170.0118	-9.3
	$C_3H_8NO_5P$	$[M+H]^+$		170.0213	0.2
	$C_4H_9N_3O_2$	$[M+K]^+$		170.0326	11.5
	$C_5H_9NO_3$	$[M+K]^+$		170.0214	0.3
methyladenine	$C_6H_7N_5$	$[M+Na]^+$	172.0503	172.0594	9.1
adenine / guanine	$C_5H_5N_5$	$[M+K]^+$	174.0245	174.0176	-6.9
	$C_5H_5N_5O$	$[M+Na]^+$		174.0386	14.1
methylguanine / phenylalanine	$C_6H_5NO_4$	$[M+Na]^+$	188.0548	188.0554	0.6
	$C_9H_{11}NO_2$	$[M+Na]^+$		188.0682	13.4
methoxytryptophan	$C_{12}H_{11}NO_3$	$[M+Na]^+$	257.0960	257.0897	-6.3
methyldeoxycytidine / glycerophosphocholine	$C_{10}H_{15}N_3O_4$	$[M+K]^+$	280.0689	280.0694	0.5
	$C_8H_{20}NO_6P$	$[M+Na]^+$		280.0920	23.1
CMP-glycoloylneuraminate	$C_{20}H_{31}N_4O_{17}P$	$[M+H]^+$	631.1309	631.1495	18.6
PC(32:1) / PE(35:1)	$C_{40}H_{78}NO_8P$	$[M+H]^+$	732.5248	732.5538	29.0
PC(34:4) / PE(37:4)	$C_{42}H_{76}NO_8P$	$[M+H]^+$	754.5208	754.5381	17.3
PC(O-34:5)	$C_{42}H_{76}NO_7P$	$[M+Na]^+$	760.5369	760.5251	-11.2
PC(33:2)	$C_{42}H_{82}NO_7P$	$[M+K]^+$	782.5303	782.5460	15.7
PC(36:1)	$C_{44}H_{86}NO_8P$	$[M+H]^+$	788.5903	788.6164	26.1
PC(35:3) / PE(38:3)	$C_{43}H_{80}NO_8P$	$[M+K]^+$	808.5430	808.5253	-17.7
PC(35:2) / PE (38:2)	$C_{43}H_{82}NO_8P$	$[M+K]^+$	810.5681	810.5773	9.2

Table S1. Tentative assignment of 7 significant peaks in buccal epithelial cells from based on LAESI-MS spectra (see Figure 4a) acquired in plume collimation experiments.

Metabolites and Lipids	**Formula**	**Ion**	$m/z_{meas.}$	$m/z_{calc.}$	**Δm (mDa)**
dodecenoic acid	$C_{12}H_{22}O_2$	$[M+H]^+$	199.1745	199.1698	-4.7
hexose	$C_6H_{12}O_6$	$[M+K]^+$	219.0075	219.0271	19.6
oxohexadecanoic acid	$C_{16}H_{30}O_3$	$[M+H]^+$	271.2054	271.2273	21.9
glutamyl-leucine	$C_{11}H_{20}N_2O_5$	$[M+K]^+$	299.1085	299.1009	-7.6
disaccharide	$C_{12}H_{22}O_{11}$	$[M+Na]^+$	365.1038	365.1060	2.2
galactinol dihydrate	$C_{12}H_{26}O_{13}$	$[M+K]^+$	417.0932	417.1010	7.8
trisaccharide	$C_{18}H_{32}O_{16}$	$[M+Na]^+$	527.1738	527.1588	-15.0

REFERENCES

(1) Nemes, P.; Vertes, A. *Anal. Chem.* **2007**, *79*, 8098-8106.